IEEE Access
Multidisciplinary | Rapid Review | Open Access Journal

Received 7 September 2023, accepted 26 October 2023, date of publication 8 November 2023,
date of current version 20 November 2023.

Digital Object Identifier 10.1109/ACCESS.2023.3330439

RESEARCH ARTICLE

Hybrid Excitable Spiking Neural Network for Cardiovascular Disease Prediction

ASIF MEHMOOD AND MUHAMMAD JAVED IQBAL
University of Engineering and Technology, Taxila, Taxila 47080, Pakistan
Corresponding author: Asif Mehmood (asif.mehmood@students.uettaxila.edu.pk)

ABSTRACT The functional interactions between the brain and heart through analysis of electrical activity (EEG and ECG) provide effective bio-markers for cognition, emotions, and morbidity. Conventional computational models designed for the brain and heart can be modified to understand the bidirectional interactions as the brain-heart interface for further clarification and treatment of morbidity. In this work, hybrid excitable cell model of neuron and cardiac myocyte is proposed and simulated with adrenergic features. The accuracy of proposed model observed 86% in terms of coincidence factor and 83% in terms of firing rate coefficient when compared with state-of-the-art computational models. The proposed model extended to the network of cardiac myocytes and electrical activity is recorded. The major findings of the study include i. Cardiac action potential heterogeneity is a significant factor in heart rate variability. ii. Spiking neural networks can accurately predict heart rate variability in real time from electrophysiological data of the cardiac network. iii. The electrical activity of the heart can be monitored and controlled by processing electrophysiological data of cardiac myocytes with spiking neural networks coupled with ion channels as voltage regulators to reduce the risk of cardiac morbidity and mortality. This work provides the initial phase of the brain-heart interface as a tool for the diagnosis of cardiac morbidity in real-time. The recent advancements in nano and bioelectronics will make it possible to deploy a brain-heart interface as a nano-chip to monitor and control the electrophysiological abnormality of the brain and heart by integrating nano-regulators with ion channels for stimulation.

INDEX TERMS Artificial intelligence, feature extraction, Izhikevich model, neural networks, neurocomputational features.

I. INTRODUCTION

The prime focus of computational neuroscience is the investigation of the long-standing question, of how the brain processes information accurately [1]. For this purpose, simulation of a large-scale brain neural network is performed by computational models to extract animal behavior at different levels of abstraction [2]. Traditionally, computational models follow the hierarchy where the brain controls the rest of the body. However, in reality, the responses of other organs can affect the functionality of the brain as well. Thus, communication between the brain and organs is bidirectional and dynamic in nature [3], [4].

Besides the central nervous system, another significant system is the autonomic nervous system, mainly related to the heart in terms of sympathetic and parasympathetic coordination. The brain monitors and controls the complex behaviors of the heart in real-time with reasonable accuracy. The electrical response of the heart approaching the brain through nerves contains sufficient information to extract all the features of heart functionality. Hence, simulation of the brain-heart interface can discover the information processing mechanism of the brain effectively, because their behavior is well examined in different studies [5], [6]. Simulation of the brain-heart interface by computational models will reduce the time-consuming, expensive, and ethically prohibitive experiments regarding the animal behavior recorded during complex tasks related to vision, speech, motor control, cognition, and intelligence [7]. For this purpose, there is

The associate editor coordinating the review of this manuscript and approving it for publication was Valentina E. Balas.

© 2023 The Authors. This work is licensed under a Creative Commons Attribution-NonCommercial-NoDerivatives 4.0 License.
For more information, see https://creativecommons.org/licenses/by-nc-nd/4.0/

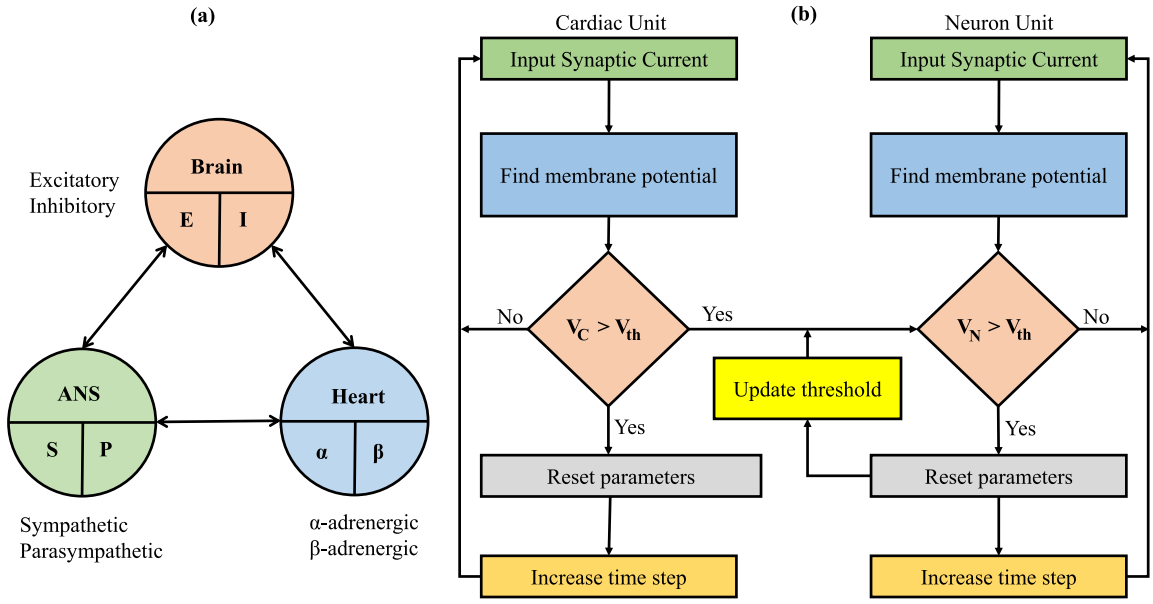


FIGURE 1. Functional hierarchy of brain-heart interactions: (a) Communication between brain (excitatory and inhibitory neurons) and heart (α and β-adrenergic receptors) by the autonomic nervous system (sympathetic and parasympathetic). (b) Communication between neuron and cardiac myocyte by electrical spikes.

need of computationally simple, efficient, and bio-physically accurate model of brain and heart.

In past few decades many attempts have been initiated to model the large scale spiking neural network of brain-heart interface. These studies can be categorized as quantitative and qualitative, based upon scalability of neural network, complexity of synaptic connections, speed of network excitation and integration of different neural networks during complex tasks. These studies concluded that adaptive models are more accurate than conventional computational models when compared with experimental datasets at cell level [8]. Hence, to discover the communication pathways between the brain and the autonomic nervous system, adaptive computational models are more suitable than classical models. In principle, communication between brain and heart is of four types: *neurologically* (by nerve impulses), *biochemically* (neurotransmitters such as NMDA, GABA, AMPA and hormones such as adrenaline and nor-adrenaline), *biophysically* (through pressure pulses) and *energetically* (by electromagnetic interactions) [9]. In this work, our focus is neurological and biochemical communication, as the rest of the pathways are being explored in detail by wearable devices.

To model the behavior of neuron and cardiac myocyte, we proposed hybrid excitable cell (HEC) model. This model belongs to the class of quadratic integrate and fire model. However, adrenergic and hormonal currents are the unique features of the proposed model. We first examined state-of-the-art computational models to predict neural responses in agreement with the dataset. However, we observed that the spike firing responses of computational models not converging the dataset. This drawback occurred due to linear membrane potential and threshold formulation. This enables us to modify the computational models and proposed model in a more sophisticated manner to integrate new parameters related to neurotransmitters and hormones. These features are the prime motivation behind the proposed model to be unique and novel in terms of α and β adrenergic receptors, responsible to control tachycardia (fast heart rate) and bradycardia (slow heart rate).

The functional hierarchy of proposed model to describe the brain-heart interface is illustrated in Figure 1. Figure 1(a) elucidates the interaction between the brain and heart via the autonomic nervous system (ANS). The two-way arrow represents a bidirectional communication signal, sharing information between organs [10]. In the brain, two variants of neuron, excitatory and inhibitory were simulated, while for ANS sympathetic and parasympathetic neurons were simulated, and finally, in the heart, α-adrenergic and β-adrenergic receptors (variants of adrenaline and nor-adrenaline hormones) dependent cells were simulated [11]. Figure 1b depicts the interaction between neuron and cardiac myocyte by action potential pulses V_N and V_C respectively. Whenever cardiac myocyte fires action potential V_C, depending upon firing frequency (tachycardia or bradycardia), α-adrenergic or β-adrenergic receptors are activated which are associated with hormonal variants of adrenaline and nor-adrenaline. These receptors fire neurons in ANS and feedback current

is communicated to the brain. Thus, control signals are generated by the brain and ANS to control the heart rate via α-adrenergic and β-adrenergic receptors [12].

The major contributions of this work are the following:

- A unified model of excitable cells is proposed by integrating the features of adaptation, adrenergic receptors, and neurotransmitters to previously reported quadratic integrate and fire model to simulate the behavior of the individual cell in response to time-varying input current.
- The electrical response of cardiac myocytes of different species is simulated by the proposed model.
- Proposed model extended to the autonomic nervous system of the heart with sympathetic and parasympathetic variants, responsible for heart rate variability.

The rest of the paper is organized as follows. A brief literature review is provided in Section II. Details of our proposed approach to model the neuron and cardiac myocyte are described in Section III. Section IV elucidates experimental settings and datasets, baseline approaches, and performance evaluation measures. Section V provides results and discussion along with comparison and Section VI contains conclusions and future work.

II. LITERATURE REVIEW

Modeling of the brain involves the complex model parameters (non-linear in nature) at the single-cell and network-level of neurons. To construct a biologically detailed model (covering neurocomputational features and morphology) of the brain, a comprehensive model of a neuron is required. The class of models defined by Hodgkin and Huxley type neuron are bio-physically meaningful, but computationally complex. Such models contain a set of non-linear differential equations to evaluate the membrane potential instantaneously [13]. The solution of a set of non-linear differential equations is usually performed by numerical methods. The complexity of such models not only depends upon model parameters but also on the numerical techniques imposed [14]. Although quantitative models are accurate and capture the realistic dynamics of biological neurons, yet are not able to simulate the large-scale brain neural network due to the increasing complexity of the number of neurons.

To ensure the computational efficiency and bio-physical plausibility, computational models of neuron proposed. These models can capture the behavior of spiking neurons with the same type of input current as injected into the biological neuron. The most popular and simplest computational model is called integrate and fire (I&F) neuron by considering neuron as the combination of resistance and capacitance [15]. Although, the I&F neuron is simple, yet very far apart from the most common neurocomputational features of spiking neurons. The improvements in the I&F model resulted in Izhikevich model (2003), proposed based on the curve fitting technique.

Although, computational models are efficient and suitable for large scale brain simulation, yet have limitations. For the neocortex, single-cell models are Izhikevich model (2003), Pospischil et al. (2008), Hay et al. (2011) and Smith et al. (2013) while network models are Brunel (2000), Truab et al. (2005), Potjans and Diesmann (2014), Markaram et al. (2015), Sadeh et al. (2017) and Dura-Bernal et al. (2017) [16]. For the cerebellum, a very comprehensive single-cell model is proposed by Solinas et al. (2017) and network models are Maex and De Schutter (1998), Vervaeke et al. (2010), and Cayco-Gajic (2017). Pinsky and Rinzel (1994), Migliore et al. (2005), and Ferguson et al. (2013) proposed single-cell models for the hippocampus while Wang and Buszaki (1996) and Bezaire et al. (2016) proposed a network model of hippocampus [17]. These models are either extension of the basic integrate and fire model or a combination of conductance-based models and computational models. Computationally efficient models are capable to replicate enriched behaviors of spiking neurons, however, spike-time-indices are compromised in the presence of time-varying synaptic input current.

A. ADAPTIVE REGIONAL-BASED MODELS

International competition on quantitative neuron modeling addressed the adaptive behavior of neurons [18]. Later on, adaptive models of neurons have been proposed with model parameters in correlation with biological neurons [19]. Adaptive models are more accurate and reliable than existing computational models in terms of accurate spike estimation. Such models include multi-scale adaptive threshold (MAT), augmented multi-scale adaptive threshold (AMAT), generalized leaky integrate and fire (GLIF) and extended generalized leaky integrate and fire (EGLIF) [20], [21], [22]. AMAT model contains a set of four differential equations while the EGLIF model contains a set of three differential equations. Moreover, both models can simulate single-cell behavior accurately with a limited number of neurocomputational features and cannot be extended to large-scale brain network level [23]. Izhikevich model depicted almost all known neurocomputational features of spiking neurons in response to a direct current stimulus. However, at the large-scale network level where synaptic connections introduce time-varying current, Izhikevich model tends to increase the spike timing and firing rate perturbation [24]. Hence, a comprehensive neuron model with enriched neurocomputational features and network dynamics similar to biological neurons is required.

III. MATERIALS AND METHODS

This research is limited to the study of dynamics of the brain at the single-cell level in terms of coincidence factor and normalized correlation coefficient (level II) and at the network level in terms of firing rates (level III). Biophysical details and anatomical features of neurons (level I) were not included due to the limitations of the model implemented. Thus, we merely need to detect fluctuations within the frequently activated regions of the brain by extracting prevalent spatial distribution patterns of neurons.

Simulation of the brain at the network level comprises multi-typed objects (layers and regions) and links

(axon and synaptic connections) between them. Without loss of generality, it can be defined as a directed network $G_A = (S_c, C_x, S_p, I_g)$, where S_c elucidates scalability of the network, is the set containing the number of neurons and their synaptic connections, C_x (complexity) is the set of parameters used in brain simulation such as capacitance, resistance, neurotransmitters (GABA, NMDA, AMPA, etc.), extracellular and molecular interactions, S_p (speed) deals with the set of synaptic connections and synaptic weights (as described by Hebbian learning) and I_g (integration) is the set of models with top-down or bottom-up architecture of different types of cells such as lugaro, Purkinje, basket, candelabrum, granule, stellate cells, etc. The particular computational structure of neurons introduced in this paper to update the value of instantaneous neurons assumes two types of nodes: i) target types (center) and ii) attribute types. The relation between target and attribute types is defined by the finite difference method (as the dataset is discrete). In particular, for brain stimulation, only scalability as the target type is assumed, while complexity, speed, and integration are left out for future work.

Given a G_A, a set of brain regions G_B=(cortex, hippocampus, thalamus, cerebellum, basal ganglia, olfactory bulb, ...) can be defined, with vertex type $G_V = \{X, X^c\}$, following the fixed point neuron computation, an object neuron N is defined as $N = (V_t, E_t)$, where $V_t \in G_B$ called an action potential and E_t is an edge between vertices called an axon. Depending upon V_t, different neurocomputational features can be extracted V_t=(spiking, bursting, class-1, class-2, ...). It should be noted that X and X^c are regional and cross-regional objects respectively. In brain simulation, the target object (scalability) co-evolves with its linked attribute objects defined by G_B. For example, in a certain timestamp, attribute scalability may have regional (cortex to cortex) or cross-regional (cortex to thalamus) influence on animal behavior concerning V_t (spiking or bursting, etc.).

The brain stimulation at the cell level adheres to different types of objects (neurotransmitters) and links (neurocomputational features). All these objects and links in the network are usually connected with time. Hence a dynamic network can then be split into a sequence of a network according to that time information in terms of firing rates and gathered in the spatial domain. A network sequence is, therefore, denoted as $G_B = (G_1, G_2, G_3, \ldots G_T)$, where $G_t = (V_t, E_t)$ is the network linked with time window t.

A. HYBRID EXCITABLE CELL MODEL

Hybrid Excitable Cell (HEC) model of neurons for large-scale brain simulation to estimate membrane potential can be expressed by Equations 1, 2, 3, 4, and 5. We assume a static threshold ($V_{th} = \theta$) for the first spike and update it for the next iterations.

$$v' = k(v - V_r)f(v - V_{th}) - u + RI \tag{1}$$
$$u' = a(bv - u) \tag{2}$$

where current I is the combination of neurotransmitter current I_n, hormonal current I_h, and somatic current I_s.

$$I = I_n + I_h + I_s$$
$$I_n = I_{NMDA} + I_{AMPA} + I_{GABA} + \ldots$$
$$I_h = I_\alpha + I_\beta + \ldots$$

I_s is random in nature and cannot be formulated mathematically. Each term of neurotransmitter and hormonal current is defined by membrane potential v, gating potential V_x, mean gating conductance $\bar{g}_x$, index of most recent spike t_s, a neurotransmitter or hormonal time constant τ_x and can be expressed as:

$$I_x = \bar{g}_x(v - V_x)e^{(t_s - t)/\tau_x} \tag{3}$$

where $\bar{g}_x$ and V_x are assumed as constant for simplicity, however, in practice their values are dynamic. Readers interested to find details of these parameters are encouraged to consult [25]. The after-spike reset values of membrane potential are:

$$\text{If } v \geq V_{th}\,; \text{ then } v = \begin{cases} V_p & \forall\, t \\ V_r & \forall\, (t+1) \end{cases} \tag{4}$$
$$V_{th} = Ae^{(t_s - t)/\tau} - \theta \tag{5}$$

where v describes the membrane potential of the neuron, V_{th} is threshold potential, f is the neural firing parameter to determine regular and fast-spiking, u is membrane recovery parameter and updated after each spike by $u \leftarrow u + d$, R is membrane resistance, V_p is the peak value of spike ($40mV$), V_r is resting state of membrane potential ($-80mV$), A is constant, t_s is the time of most recent spike, τ is membrane time constant and θ is a constant value of threshold ($-35mV$) when the cell is quiescent.

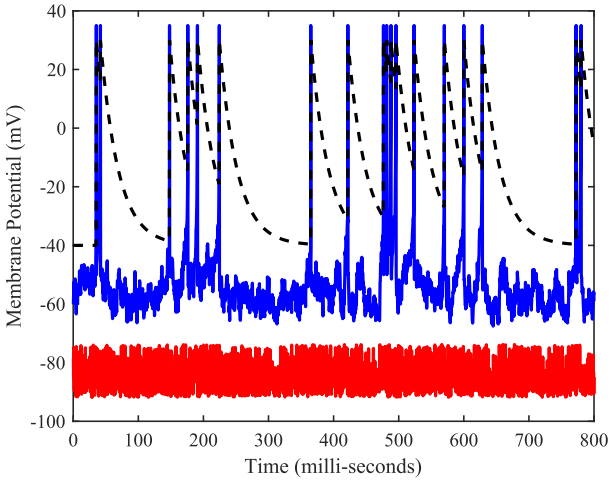


FIGURE 2. HEC model (blue), threshold function (black), and input current (red).

For implementation of model described by Equations 1, 2, 3, 4 and 5, Euler method is utilized to evaluate membrane

potential as $v(k+1) = v(k)+hv(\acute{k})$, where ($\acute{}$) illustrates first-order derivative with respect to time. The spiking behavior of the HEC model is delineated in Figure 2 in response to the time-varying synaptic current and the MATLAB code of Figure 2 is provided in supplementary material for illustration. Initially, the threshold (represented by the black line in Figure 2) remains static unless the first spike is fired. For the next iteration, the adaptive threshold is evaluated, defined by Equation 4 [21]. An action potential spike will be generated when membrane potential (plotted in blue solid line in Figure 2) touches the threshold. The threshold is increased by a fixed amount (A in this case) after each firing. Thus, the variable threshold observed in biological neurons can be confirmed by assuming the adaptation parameter defined in Equation 5. Readers interested to find the details of model implementation and a detailed description of parameters can consult [26].

B. CARDIAC MYOCYTE

The electrical activity in the heart is primarily initiated by pace-making cells in the sinoatrial (SA) node and atrioventricular (AV) node [27]. The computational model for membrane potential of cardiac myocyte (from resting to depolarization) in the simplest form can be written as:

$$V' = k(V - V_r)f(V - V_{th}) - u + V_{AV} + V_{SA} + RI \quad (6)$$

$$u' = a(bV - u) \quad (7)$$

V_{AV} = Potential generated by AV node = $V_\beta e^{-(t-n\tau)/T_k}$
V_{SA} = Potential generated by SA node = $V_{Ca}e^{-(t-n\tau)^2/T_{Ca}}$
$I = I_{Na} + I_{NaL} + I_{to} + I_{CaL} + I_{Kr} + I_{Ks} + I_{K1} + I_{NaCai} + I_{NaCass} + I_{NaK} + I_{Kb} + I_{Nab} + I_{Cab} + I_{pCa} + J_{leak} + J_{rel} + J_{tr} + J_{up} + I_{stim}$ After spike potential, from hyper-polarization to resting potential can be approximated as:

$$\text{If } V \geq V_{th}\text{; then } V = \begin{cases} V_\beta e^{-(t-n\tau)/T_K} & \forall\, t \\ V_{Ca}e^{-(t-n\tau)^2/T_{Ca}} & \forall\, (t+1) \end{cases} \quad (8)$$

$$\text{If } V \leq V_{APD_{50}}\text{; then } V = \begin{cases} V_r e^{-(t-n\tau)/T_L} & \forall\, t \\ V_\alpha e^{-(t-n\tau)/T_{Na}} & \forall\, (t+1) \end{cases} \quad (9)$$

Parameters in Equations 6, 7, 8 and 9 are defined as n is the number of cardiac spikes, f is cardiac myocyte firing parameter, τ is the duration of one cardiac action potential, V_β is potential generated by β-adrenergic receptors for activation of cardiac myocyte, V_{Ca} is potential due to calcium handling via alterations of trans-membrane currents and intracellular calcium homeostasis, V_α is potential generated by α-adrenergic receptors for inhibition of cardiac myocyte, T_k is time constant for potassium channels, T_{Ca} is the time constant for calcium channels, T_{Na} is the time constant for sodium channels and I is stimulation current to initiate a cardiac action potential. Readers interested to find details of ion channel current dynamics I are encouraged to consult [10], however, a quick review with MATLAB code is provided for illustration in the supplementary material.

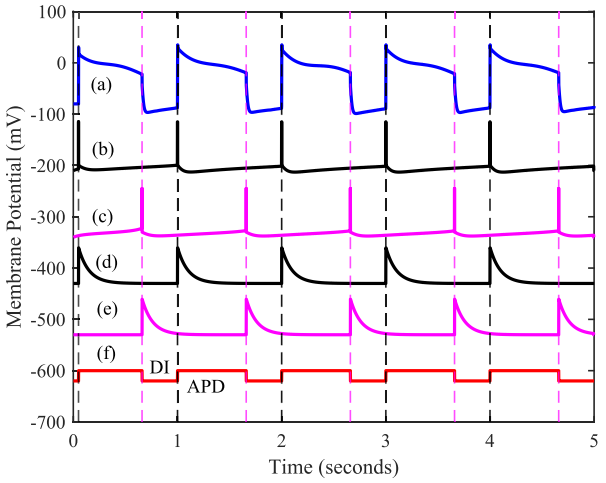


FIGURE 3. a) Cardiac action potential spikes (blue) b) β-adrenergic dependent neuron (black) c) α-adrenergic dependent neuron (magenta) d) β adrenergic potential e) α adrenergic potential f) cardiac myocyte electrical activity scaled in digital form (red).

The cardiac action potential depicted in Figure 3a is generated by sodium, potassium, calcium, and leakage ions by implementing Equations 6, 7, 8 and 9 by Euler method. Due to the inward movement of fast sodium ions ($V_\alpha e^{-(t-n\tau)/T_{Na}}$), the membrane potential of cardiac myocyte rapidly increases from −80 millivolts to +20 millivolts. This activates β-adrenergic receptors (defined by Equation 3) along with potassium ($V_\beta e^{-(t-n\tau)/T_K}$) and calcium ($V_{Ca}e^{-(t-n\tau)^2/T_{Ca}}$) ion channels (Equation 8) to trigger the neuron as represented by the black solid line in Figure 3b. Calcium channels gently increase the influx of calcium ions, as a result, a plateau phase of the cardiac action potential is formed. When potential drops from −20 millivolts, leakage channels ($V_r e^{-(t-n\tau)/T_L}$) are opened and cardiac action potential drops towards the negative apex. As a result, α-adrenergic receptors (Equation 3, Figure 3e) are activated [29] to trigger the neuron as represented by the magenta solid line in Figure 3c. Hence, the electrical response of cardiac cells in the form of feedback current is generated to stimulate the neurons of the autonomic system as elucidated by the red solid line in Figure 3f. The time interval when cardiac action potential remains above the threshold potential is called action potential duration (APD), while the interval below threshold potential is called diastolic interval (DI). The relation between APD and DI is termed a restitution function. Cardiac heterogeneity depends upon the depolarization protocols of membrane potential defined by 90%, 50% or 30% depolarization, denoted by APD_{90}, APD_{50} or APD_{30} respectively. Restitution function represents the cardiac electrical activity in terms of tachycardia and bradycardia [12]. The cardiac myocyte model can be extended to different species depending upon

TABLE 1. Values of model parameters for simulation of cardiac myocytes of different species [28].

Parameter	Human	Guinea Pig	Rabbit	Mouse	Rat
a	0.03	0.03	0.03	0.03	0.03
b	-6	-2	-2	-2	-2
C	50μF	50μF	50μF	100μF	50μF
d	25	20	5	4	10
k	0.5	0.7	0.5	0.5	0.7
f	0.25	0.15	0.2	0.25	0.5
V_α	-60mV	-46mV	-41mV	-60mV	-60mV
V_β	70mV	70mV	70mV	70mV	70mV
V_{Ca}	45mV	30mV	25mV	0	0
R_k	5MΩ	5MΩ	5MΩ	3.8MΩ	0.2MΩ
R_{Ca}	5MΩ	5MΩ	5MΩ	0	0
R	95MΩ	95MΩ	95MΩ	95MΩ	0

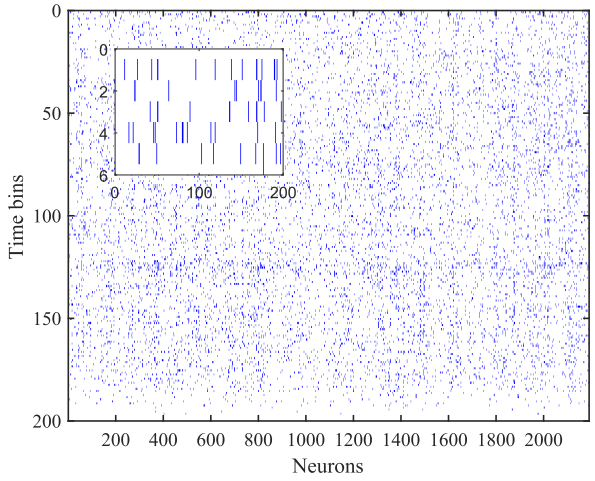


FIGURE 4. Neural ensembles representation of one trial of dataset (2191 × 217) out of 14 trials. The box depicts a zoomed-in version of neural ensembles of 200 neurons over 6 time-bins.

the nature of electrophysiological responses as depicted in Table 1.

IV. EXPERIMENTS

A. EXPERIMENTAL SETTINGS AND DATASET

This work is purely related to the simulation by computational models, therefore no experiment was conducted on animal subjects. However, previously recorded data of mouse brain assumed as a dataset for validation of computational models [20]. The dataset contains experimental recordings of 2191 neurons of the mouse brain and comprises a three-dimensional matrix $2191 \times 14 \times 217$ (2191 neurons, 14 trials, 217-time bins). Each trial is analyzed in the time domain to extract neural ensembles of 2191 neurons as exhibited in Figure 4. Each vertical line in Figure 4 (zoomed-in box) illustrates the firing of a neuron.

B. BASELINE APPROACHES

For fair quantitative comparison, baseline models are selected from the same class of neurons, that is, integrate and fire neurons. A brief description of baseline approaches is provided below.

1) GENERALIZED LEAKY INTEGRATE AND FIRE (GLIF) MODEL

The membrane potential v of GLIF model can be expressed as [22]:

$$v' = \frac{1}{C_m}\left(\frac{C_m}{\tau_m}(v - V_{dep}) - V_{adap}\right) + IR$$
$$V'_{adap} = k_1(v - V_{dep}) - k_2 V_{adap}$$

C_m is membrane capacitance,R is membrane resistance, $\tau_m = RC_m$, k_1 and k_2 are adaptation constants. Spike generation of the GLIF model is illustrated in Figure 5(a) where input current is delineated in Figure 5(b).

2) MULTI-SCALE ADAPTIVE THRESHOLD (MAT) MODEL

The membrane potential v of MAT model with adaptive threshold V_{th} can be expressed as [20]:

$$v' = \frac{1}{\tau_m}(v - E_L) + \frac{1}{C_m}I$$
$$V_{th} = \sum_k H(t - t_k) + \beta \int_{-\infty}^{t} K(s)v'(t - s)ds + w$$
$$H(t) = (\alpha_1 e^{-t/\tau_1} + \alpha_2 e^{-t/\tau_2})h(t)$$
$$K(s) = se^{-s/\tau_v}h(s)$$

$h(t)$ is unit step function. An action potential spike is generated at t_k if $v(t_k) \geq V_{th}(t_k)$. After a spike is emitted at t_k, the neuron holds refractoriness property, and cannot fire a new spike until the refractory period $(t_k + \tau_{ref})$ is passed. The response of the MAT model to input random current is depicted in Figure 5(c).

3) QUADRATIC INTEGRATE AND FIRE (QIF) MODEL

QIF model can be expressed as [26]:

$$v' = 0.04v^2 + 5v + 140 - u + I$$
$$u' = a(bv - u)$$

With after-spike reset values of:

$$\text{If } v \geq V_{th}\text{ ; then } v = \begin{cases} V_p & \forall\, t \\ V_r & \forall\, (t+1) \end{cases}$$

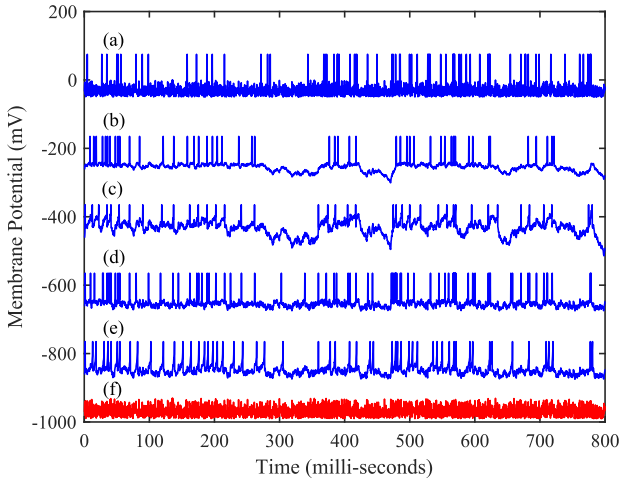


FIGURE 5. (a) Dataset (b) GLIF (c) MAT (d) QIF (e) HEC Model (f) Input current.

An action potential spike is generated at t_k if $v(t_k) \geq V_{th}$ and parameters are initialized to resting state. The membrane potential initiated by the QIF model by random input current is manipulated in Figure 5(d).

C. PERFORMANCE EVALUATION MEASURES

1) COINCIDENCE FACTOR

Performance of HEC model (Figure 5e) against experimental data (Figure 5a) can be evaluated by coincidence factor Γ [21], defined as:

$$\Gamma = \frac{2(N_{coinc} - \langle N_{coinc} \rangle)}{N(N_{model} + N_{data})} \tag{10}$$

where N_{coinc} is the number of spikes coinciding with experimental data, $\langle N_{coinc} \rangle = 2\nu\Delta N_{data}$ is the average number of coincidence of Poisson spikes generated in equivalence of model frequency, N_{model} is the number of spikes predicted by the HEC model and N_{data} is the total number of spikes in experimental data, factor $N = 1 - 2\nu\Delta$ normalizes gamma factor to a maximum value of 1, $\nu = N_{data}/T$ is spike generation rate with T as the duration of the experiment, Δ is the size of the window on time axis within which two spikes fired would be assumed as coincident. The value of the coincidence factor as unity ($\Gamma = 1$) depicts the exact convergence of the model to experimental data.

2) FIRING RATE COEFFICIENT

For a large number of neural ensembles, evaluation of coincidence factor is cumbersome and may encounter inappropriate results due to bias sensitivity [30]. In such cases, the normalized correlation coefficient for the firing rate of the network is a better choice for performance evaluation and can be defined as:

$$\eta = \frac{Cov(x, y)}{\sqrt{Var(x)Var(y)}} \tag{11}$$

where x stands for experimental data, y elucidates predicted data. η is less sensitive to bias and only deals with neural variability because the mean is subtracted in the evaluation of covariance and variance. The value of η approaching 1 indicates the exact convergence of the model to experimental data while approaching 0, results in poor prediction.

V. RESULTS AND DISCUSSION

In the following subsection *Single-Cell Performance*, we compare the spike train of the dataset with the spike train generated by QIF, MAT, GLIF, and HEC model and calculate the performance in terms of gamma factor defined by Equation 10. In the second subsection *Network Performance*, we study the variability of spike train at the network level in terms of the firing rate coefficient defined by Equation 11. As the firing rate is a cumulative response of the network at a certain timestamp, thus deviation is expected (adorned in Table 2) at the cost of temporal properties available at the cell level. In the third subsection *Cardiac Myocyte*, the HEC model is tuned to replicate the electrical response of a single cardiac myocyte. In subsection *Heart Rate Variability*, the HEC model is extended to the autonomic nervous system of the heart at the network level. Depending upon the values of spike timing, cardiac restitution function is plotted, and the heart rate variability of the cardiac network is determined.

A. SINGLE-CELL PERFORMANCE

The electrical activity of the mouse brain is assumed as the dataset for validation of computational models [20]. The dataset contains experimental recordings of 2191 neurons of the mouse brain and comprises a three-dimensional matrix 2191 × 14 × 217 (2191 neurons, 14 trials, 217-time bins). The model data with the same dimensions as the dataset is predicted by HEC, MAT, GLIF, and QIF models (described in Section III, Figure 5) that can yield quantitative predictions about the spike train of the cell. To establish a fair quantitative comparison between dataset and model predictions, the intrinsic reliability of the target neuron is evaluated in terms of coincidence factor Γ. Equations 1, 2, 3, 4 and 5 are implemented for HEC model to evaluate membrane potential. For a valid quantitative comparison, dimensions of predicted data were restricted to the dataset as (2191 × 14 × 217). To evaluate the coincidence factor, the following procedure is implemented:

i) Define a mask vector for each model containing five elements to ensure the precision of ±2 elements on either side of the dataset element being compared, starting at the central element.

ii) Load mask vector with model data of five elements containing spikes of data.

iii) Select an element from the dataset and compare it with mask vector elements starting from the central element.

iv) If the dataset is matched with any of five mask elements, increase the coincidence counter by 1.

v) For every dataset element, five searches for coincidence are required.

We find that the HEC model yields a prediction of spike firing time with up to 86% of spike timing correct (within ±2 elements) when compared with QIF, MAT, and GLIF models with 77%, 73% and 69% prediction accuracy respectively as elaborated in Table 2. The MATLAB code file (gamma.m) of computation for each neuron with 217 data points, is provided in supplementary material for illustration. Readers are encouraged to find details of the method in [21] and [31].

B. NETWORK PERFORMANCE

The method of mean firing prediction at the neural network level is a good indicator of performance evaluation as the characteristics of individual cells are collectively evaluated, however, temporal features are lost. Large-scale brain simulation involves accurate connections between neurons to converge the experimental results. However, such exact connections between neurons are not known at this time. Hence, large-scale brain simulation relies on sparsely coupled neurons as demonstrated by [2].

The performance of rate models in response to realistic spike trains can be analyzed by Equation 11. The dataset contained 2191 neurons, and 217 time-bins recorded during 14 trials, characterized by point neurons. Dataset ($N_{neurons} \times N_{trials} \times N_{time}$) is decomposed into the individual trial ($N_{neurons} \times N_{time}$) and spikes of 2191 neurons across each time-bin are added. The results of each trial comprise 217 elements containing firings of 2191 neurons in each element. Equation 11 is implemented over 14 trials containing 217 elements per trial of firing data and results are illustrated in Table 2. A similar procedure is adopted for model data containing 2191 neurons, 217-time bins, and 14 trials. Details of computation along with MATLAB code are provided in the supplementary material for model validation. As the firing rate evaluates cumulative firings of neurons instantaneously instead of individual spikes, hence, accuracy is compromised due to the elimination of mean from each trial. Statistical analysis of conventional computational models (Table 2) in response to the dataset suggests that the HEC model is suitable for the simulation of the brain-heart interface.

C. HEART RATE VARIABILITY

Heart rate variability (HRV) is the variation of heartbeats or variance of the difference of inter-beats interval (IBI) in time domain [32]. Statistically, HRV is referred to as the root mean square of successive difference (RMSSD) between normal heartbeats. Clinically, HRV is determined by RR interval (Difference between two consecutive R waves) from the ECG signal. This parameter is related to the monitoring of an individual's cardiac health. A higher value of HRV indicates a healthy heart, more resilience to changes, and vice versa. HRV is controlled by the autonomic nervous system, which constantly communicates with the hypothalamus, and a control signal is sent to the rest of the body to stimulate or relax [33]. Conventional methods (Electrocardiogram (ECG), Electrodermal activity (EDA), photoplethysmography (PPG), and respiration (RESP) analysis) to estimate HRV are efficient in terms of accuracy, reliability, and usefulness as an indicator of cardiac health [29], however, are not capable of monitoring for long period. Hence, we need to discover efficient methods to predict, monitor and control HRV with reasonable accuracy by processing raw electrical signals generated by the heart directly in real-time.

Simulation of the brain-heart interface can be encountered by building a combination of cardiac-neural network [34]. For this purpose, a network of 1000 neurons is coupled with cardiac myocytes and activated by random synaptic currents within the range of ionic currents to study cardiac heterogeneity. The response of SA-node and AV-node reaching the cardiac myocytes along with adrenergic receptors play a vital role to generate heartbeats [35]. For simplicity, the response of adrenergic receptors is generated by spike occurrence of cardiac myocytes because at this stage our focus is to generate cardiac impulses in the form of electrophysiological signals to process by spiking neural network.

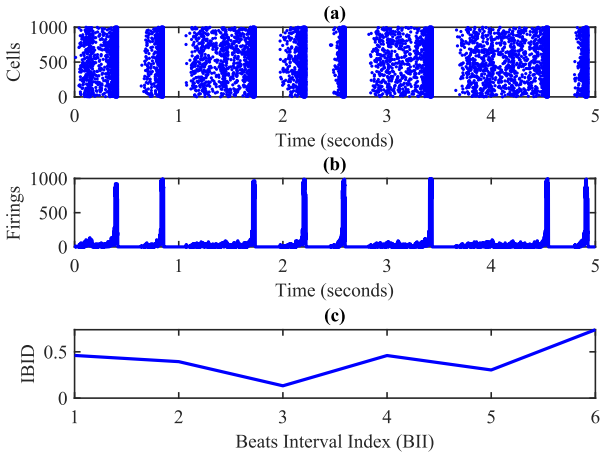


FIGURE 6. (a) A network of 1000 neurons sparsely coupled with cardiac myocytes activated synchronously and electrical activity recorded. (b) Neuron firings are superposed to estimate heartbeats. (c) Variation in heartbeats is calculated by the difference between consecutive beats.

The response of 1000 neurons coupled with cardiac myocytes is depicted in Figure 6(a). The electrical response of the neuron is instantaneous (due to the absence of plateau phase) as compared to cardiac myocyte, therefore, the firing of the neuron is represented by a dot. To develop cardiac network architecture by the computational model, we assumed regular spiking (RS) and fast-spiking (FS) cells where each cell contains 1000 synaptic connections. The convergence of the model network depends upon the intrinsic heterogeneity of the cell. For this purpose, values of parameters are assumed as $a = 0.02 + 0.8r$, $b = 0.2 + 0.05r$, $c = -65 + 15r^2$, $d = 8 - 6r^2$, where r is a random variable uniformly distributed over the interval [0,1] (RS: $r = 0$ and FS: $r = 1$), c is reset value of membrane potential and d is the step size of membrane potential recovery parameter u. The synaptic

TABLE 2. Comparison between GLIF [21], MAT [20], QIF [22], and HEC model, where for Γ, dataset implies number of spikes while for η, dataset implies cumulative firings instantaneously. MATLAB code of each model is provided in the supplementary material for illustration.

	Coincidence Factor Γ			Firing Rate Coefficient η		
Model	Dataset	Prediction	Γ	Dataset	Prediction	η
GLIF	84	48	0.692066	845	488	0.563079
MAT	84	53	0.733302	845	535	0.620518
QIF	84	58	0.774240	845	585	0.681835
HEC	**84**	**70**	**0.862579**	**845**	**708**	**0.832394**

connections matrix S with dimensions 1000×1000, contains the weights of synaptic connections, generated randomly by MATLAB function 0.5*rand(1000,1000). To introduce synaptic plasticity, we added the weights of only those neurons which fired by $I = I + sum(S(:, fired), 2)$. MATLAB code of cardiac neural network is provided in Cardiac.m file in supplementary materials. The sparseness of matrix S results in variation of cardiac restitution and hence the heart rate variability. The network model of cardiac myocytes belongs to a pulse-coupled neural network, where each firing of a cardiac myocyte is linked with a neuron and vice versa. The electrical activity of the spiking neural network in the form of beats and the effect of random variable r on the variation of the inter-beat interval is delineated in Figure 6(b).

To calculate heart rate variability, we define three vectors T, IBI, and IBID. Vector T contains time indices of beats as depicted in Figure 6(b).

$$T = [0.386\ 0.804\ 1.683\ 2.168\ 2.52\ 3.332\ 4.448\ 4.825]$$

Inter-beat interval vector is denoted by IBI and obtained by calculating the successive differences of vector T.

$$\text{IBI} = [0.418\ 0.879\ 0.485\ 0.352\ 0.812\ 1.116\ 0.377]$$

Inter-beat interval difference vector IBID is obtained by successive difference of terms of IBI vector.

$$\text{IBID} = [0.461\ 0.394\ 0.133\ 0.46\ 0.304\ 0.739]$$

The variation in inter-beat intervals is manipulated in Figure 6(c). The heterogeneity in cardiac action potential firing results in the sparseness of inter-beat intervals [36]. To ensure greater variation, the values of synaptic connection matrix S can be increased. Finally, heart rate variability is calculated by the root mean square of vector IBID.

$$\text{HRV} = \text{RMSSD(IBID)} = \text{Var(IBID)} = 40\text{ms}.$$

There is no particular value of HRV, however, it fluctuates between 30 milli-seconds to 100 milli-seconds. A high value of HRV indicates healthy heart and vice versa. The value of HRV drops with aging, however, is not an indicator of aging. The value of HRV calculated as 40 milli-seconds indicate the elderly healthy person, however, in general HRV depends upon fitness and heart rate of an individual.

During the past few decades, the development of nanotechnology in biosensor design has been very rapidly evolving. This advancement enabled intelligent wearable devices and implants to monitor internal organs for a long period in real time. As a result, many research institutions developed biosensors for medical diagnosis and patient disease monitoring from electrophysiological data. However, these sensors are not ideal for humans because biological constraints, sensor types, and data processing techniques are the main barriers to be solved in future development trends [9], [27].

The functionality of complex organs such as the brain and heart relies on bidirectional communication between entirely heterogeneous cells. Traditional implantation of electronic devices into soft tissues destructs the well-connected cellular networks by injecting micro-needle electrodes invasively [37]. To reduce cellular destruction, soft and flexible electronic electrodes, inspired by spiking neural networks, can be coupled with the main nerves carrying the information of the organ. The prime advantage of such electrodes over conventional is the acquisition of neural signals from the body without introducing noise (foreign body reaction or acute inflammatory response). Monitoring and evaluation of electrophysiological signals between the brain and organs can be used as a precursor of morbidity.

VI. CONCLUSION AND FUTURE WORK

Computer models of the brain and heart are important in the sense that allows us to perform experiments with animals virtually, which are difficult to perform physically due to ethical constraints. We can put the model in an ideal environment (noiseless) of choice that cannot be possible practically to achieve desired results. It is important to note that existing approaches to visualizing brain and heart activity need expertise. In principle, the electrical activity of the brain and heart is the superposition of signals from different organs. Hence, to process brain information accurately, we need to identify each signal separately. For this purpose, neural data must be recorded and processed by efficient methods. One way is to utilize spiking neural network architecture due to their resemblance with biological neurons.

In this work, we examined computational neuron models that can be translated into hardware. Modifications in the suitable computational model, are proposed and the model is extended to the autonomic nervous system of the heart to predict heart rate variability. Conventional methods including wearable devices and implants have limited applications to monitor and generate control signals. Here, we analyzed

heart electrophysiological traces by spiking neural networks to predict heart rate accurately. This provides confidence to utilize spiking neural network architecture not only to monitor electrophysiological data but also to deliver control signals to appropriate ion channels to stimulate artificial voltage regulators. The utilization of spiking neural networks in the design of next-generation implants will further improve the efficiency and accuracy of brain signal processing.

HRV is the prime indicator of the functionality of the autonomic nervous system (ANS) which coordinates activities of the body by an increase or decrease in blood pressure to maintain homeostasis. Any abnormality in ANS functionality can cause an increase in cardiac morbidity or mortality due to heart failure. Therefore, under extreme conditions, while cardiac arrest is being happened and ANS is out of sympathovagal balance, a dedicated system (brain-heart interface) installed as a chip in the subject is able to reset ANS towards normal condition. For this purpose, we need to process neural and cardiac data in real-time gathered from electrophysiological activity. The advantage of this technique over conventional methods is, electrophysiological data can easily be gathered and processed in real-time by spiking neural networks without deploying extra hardware. Moreover, spiking neural networks are entirely inspired by neurons, hence will be efficient while coupling with tissues without introducing noise.

COMPLIANCE WITH ETHICAL STANDARDS

Conflicts of interest: The authors declare no conflict of interest.

DATA AVAILABILITY

The datasets analyzed during the current study are publicly available with MATLAB codes on https://www.nature.com/articles/s41586-020-2130-2#data-availability.

REFERENCES

[1] D. Valencia, J. Thies, and A. Alimohammad, "Frameworks for efficient brain–computer interfacing," *IEEE Trans. Biomed. Circuits Syst.*, vol. 13, no. 6, pp. 1714–1722, Dec. 2019.

[2] E. M. Izhikevich and G. M. Edelman, "Large-scale model of mammalian thalamocortical systems," *Proc. Nat. Acad. Sci. USA*, vol. 105, no. 9, pp. 3593–3598, Mar. 2008.

[3] N. Ahmadi, T. G. Constandinou, and C.-S. Bouganis, "Estimation of neuronal firing rate using Bayesian adaptive kernel smoother (BAKS)," *PLoS ONE*, vol. 13, no. 11, Nov. 2018, Art. no. e0206794.

[4] B. Bai et al., "Deep multilayer brain proteomics identifies molecular networks in Alzheimer's disease progression," *Neuron*, vol. 105, no. 6, pp. 975–991, 2020.

[5] S. Yang, J. Wang, B. Deng, C. Liu, H. Li, C. Fietkiewicz, and K. A. Loparo, "Real-time neuromorphic system for large-scale conductance-based spiking neural networks," *IEEE Trans. Cybern.*, vol. 49, no. 7, pp. 2490–2503, Jul. 2019.

[6] C. Borges-Merjane, O. Kim, and P. Jonas, "Functional electron microscopy, 'flash and freeze,' of identified cortical synapses in acute brain slices," *Neuron*, vol. 105, no. 6, pp. 992–1006, 2020.

[7] G. T. Einevoll, A. Destexhe, M. Diesmann, S. Grün, V. Jirsa, M. de Kamps, M. Migliore, T. V. Ness, H. E. Plesser, and F. Schürmann, "The scientific case for brain simulations," *Neuron*, vol. 102, no. 4, pp. 735–744, May 2019.

[8] A. Destexhe and M. Mehta, "Properties and computational consequences of fast dendritic spikes during natural behavior," *Neuroscience*, vol. 489, pp. 251–261, May 2022.

[9] V. Catrambone and G. Valenza, "Nervous–system–wise functional estimation of directed brain–heart interplay through microstate occurrences," *IEEE Trans. Biomed. Eng.*, vol. 70, no. 8, pp. 2270–2278, Aug. 2023.

[10] F. Seibertz, M. Rapedius, F. E. Fakuade, P. Tomsits, A. Liutkute, L. Cyganek, N. Becker, R. Majumder, S. Clauß, N. Fertig, and N. Voigt, "A modern automated patch-clamp approach for high throughput electrophysiology recordings in native cardiomyocytes," *Commun. Biol.*, vol. 5, no. 1, pp. 1–10, Sep. 2022.

[11] A. Shaban, S. S. Bezugam, and M. Suri, "An adaptive threshold neuron for recurrent spiking neural networks with nanodevice hardware implementation," *Nature Commun.*, vol. 12, no. 1, p. 4234, Jul. 2021.

[12] V. Catrambone, A. Talebi, R. Barbieri, and G. Valenza, "Time-resolved brain-to-heart probabilistic information transfer estimation using inhomogeneous point-process models," *IEEE Trans. Biomed. Eng.*, vol. 68, no. 11, pp. 3366–3374, Nov. 2021.

[13] K. Amunts, J. DeFelipe, C. Pennartz, A. Destexhe, M. Migliore, P. Ryvlin, S. Furber, A. Knoll, L. Bitsch, J. G. Bjaalie, Y. Ioannidis, T. Lippert, M. V. Sanchez-Vives, R. Goebel, and V. Jirsa, "Linking brain structure, activity, and cognitive function through computation," *Eneuro*, vol. 9, no. 2, pp. 1–19, Mar. 2022.

[14] M. Corkrum, A. Covelo, J. Lines, L. Bellocchio, M. Pisansky, K. Loke, R. Quintana, P. E. Rothwell, R. Lujan, G. Marsicano, E. D. Martin, M. J. Thomas, P. Kofuji, and A. Araque, "Dopamine-evoked synaptic regulation in the nucleus accumbens requires astrocyte activity," *Neuron*, vol. 105, no. 6, pp. 1036–1047, Mar. 2020.

[15] R. Egger, R. T. Narayanan, J. M. Guest, A. Bast, D. Udvary, L. F. Messore, S. Das, C. P. J. de Kock, and M. Oberlaender, "Cortical output is gated by horizontally projecting neurons in the deep layers," *Neuron*, vol. 105, no. 1, pp. 122–137, Jan. 2020.

[16] G. Quaglio, P. Toia, E. I. Moser, T. Karapiperis, K. Amunts, S. Okabe, M.-M. Poo, J.-C. Rah, Y. D. Koninck, J. Ngai, L. Richards, and J. G. Bjaalie, "The international brain initiative: Enabling collaborative science," *Lancet Neurol.*, vol. 20, no. 12, pp. 985–986, Dec. 2021.

[17] S. Petkoski and V. K. Jirsa, "Normalizing the brain connectome for communication through synchronization," *Netw. Neurosci.*, vol. 6, no. 3, pp. 722–744, Jul. 2022.

[18] P. Gleeson et al., "Open source brain: A collaborative resource for visualizing, analyzing, simulating, and developing standardized models of neurons and circuits," *Neuron*, vol. 103, no. 3, pp. 395–411, Aug. 2019.

[19] M. Haesemeyer, A. F. Schier, and F. Engert, "Convergent temperature representations in artificial and biological neural networks," *Neuron*, vol. 103, no. 6, pp. 1123–1134, Sep. 2019.

[20] J. Igarashi, H. Yamaura, and T. Yamazaki, "Large-scale simulation of a layered cortical sheet of spiking network model using a tile partitioning method," *Frontiers Neuroinform.*, vol. 13, p. 71, Nov. 2019.

[21] R. Jolivet, F. Schürmann, T. K. Berger, R. Naud, W. Gerstner, and A. Roth, "The quantitative single-neuron modeling competition," *Biol. Cybern.*, vol. 99, nos. 4–5, pp. 417–426, Nov. 2008.

[22] R. Keerativittayayut, R. Aoki, M. T. Sarabi, K. Jimura, and K. Nakahara, "Large-scale network integration in the human brain tracks temporal fluctuations in memory encoding performance," *eLife*, vol. 7, pp. 32678–32696, Jun. 2018.

[23] M. Komarov, G. Krishnan, S. Chauvette, N. Rulkov, I. Timofeev, and M. Bazhenov, "New class of reduced computationally efficient neuronal models for large-scale simulations of brain dynamics," *J. Comput. Neurosci.*, vol. 44, no. 1, pp. 1–24, Feb. 2018.

[24] B. Li, B. N. Routh, D. Johnston, E. Seidemann, and N. J. Priebe, "Voltage-gated intrinsic conductances shape the input-output relationship of cortical neurons in behaving primate v1," *Neuron*, vol. 107, no. 1, pp. 185–196, Jul. 2020.

[25] B. Sen-Bhattacharya, S. James, O. Rhodes, I. Sugiarto, A. Rowley, A. B. Stokes, K. Gurney, and S. B. Furber, "Building a spiking neural network model of the basal ganglia on SpiNNaker," *IEEE Trans. Cogn. Develop. Syst.*, vol. 10, no. 3, pp. 823–836, Sep. 2018.

[26] E. M. Izhikevich, "Which model to use for cortical spiking neurons?" *IEEE Trans. Neural Netw.*, vol. 15, no. 5, pp. 1063–1070, Sep. 2004.

[27] R. Paudel, M. S. Jafri, and A. Ullah, "Pacing dynamics determines the arrhythmogenic mechanism of the CPVT2-causing CASQ2G112+5X mutation in a Guinea pig ventricular myocyte computational model," *Genes*, vol. 14, no. 1, p. 23, Dec. 2022.

[28] D. Moses and C. Deisy, "A survey of data mining algorithms used in cardiovascular disease diagnosis from multi-lead ecg data," *Kuwait J. Sci.*, vol. 42, no. 2, pp. 206–235, 2015.
[29] S. Ishaque, N. Khan, and S. Krishnan, "Trends in heart-rate variability signal analysis," *Frontiers Digit. Health*, vol. 3, Feb. 2021, Art. no. 639444.
[30] O. Schoppe, N. S. Harper, B. D. B. Willmore, A. J. King, and J. W. H. Schnupp, "Measuring the performance of neural models," *Frontiers Comput. Neurosci.*, vol. 10, p. 10, Feb. 2016.
[31] F. Najafi, G. F. Elsayed, R. Cao, E. Pnevmatikakis, P. E. Latham, J. P. Cunningham, and A. K. Churchland, "Excitatory and inhibitory subnetworks are equally selective during decision-making and emerge simultaneously during learning," *Neuron*, vol. 105, no. 1, pp. 165–179, Jan. 2020.
[32] V. Catrambone, G. Averta, M. Bianchi, and G. Valenza, "Toward brain–heart computer interfaces: A study on the classification of upper limb movements using multisystem directional estimates," *J. Neural Eng.*, vol. 18, no. 4, Apr. 2021, Art. no. 046002.
[33] D. Candia-Rivera, V. Catrambone, R. Barbieri, and G. Valenza, "Functional assessment of bidirectional cortical and peripheral neural control on heartbeat dynamics: A brain-heart study on thermal stress," *NeuroImage*, vol. 251, May 2022, Art. no. 119023.
[34] V. Catrambone, S. M. Benvenuti, C. Gentili, and G. Valenza, "Intensification of functional neural control on heartbeat dynamics in subclinical depression," *Transl. Psychiatry*, vol. 11, no. 1, p. 221, Apr. 2021.
[35] V. Catrambone, R. Barbieri, H. Wendt, P. Abry, and G. Valenza, "Functional brain–heart interplay extends to the multifractal domain," *Phil. Trans. Roy. Soc. A, Math., Phys. Eng. Sci.*, vol. 379, no. 2212, Dec. 2021, Art. no. 20200260.
[36] L. Quadt, H. Critchley, and Y. Nagai, "Cognition, emotion, and the central autonomic network," *Autonomic Neurosci.*, vol. 238, Mar. 2022, Art. no. 102948.
[37] D. Candia-Rivera, V. Catrambone, J. F. Thayer, C. Gentili, and G. Valenza, "Cardiac sympathetic-vagal activity initiates a functional brain–body response to emotional arousal," *Proc. Nat. Acad. Sci. USA*, vol. 119, no. 21, May 2022, Art. no. e2119599119.



ASIF MEHMOOD received the M.Sc. degree in electronics from Quaid-i-Azam University, Islamabad, Pakistan, in 2008, and the M.S. degree in computational science and engineering from the Research Center for Modeling and Simulation, National University of Sciences and Technology, Islamabad, in 2014. He is currently pursuing the Ph.D. degree with the Department of Computer Science, University of Engineering and Technology, Taxila, Pakistan. His research interests include artificial intelligence, brain simulation, human–computer interface, and neural networks.



MUHAMMAD JAVED IQBAL received the M.Sc. degree in computer science from the University of Agriculture Faisalabad, Faisalabad, Pakistan, in 2001, the M.S./M.Phil. degree in computer science from International Islamic University Islamabad, Pakistan, in 2008, and the Ph.D. degree in computer science/information technology from Universiti Teknologi PETRONAS, Malaysia, in February 2015. He is currently a HEC approved Ph.D. Supervisor and an Assistant Professor with the Computer Science Department, University of Engineering and Technology, Taxila, Pakistan. After completion of his Ph.D. studies, he has been actively involved in research. He won research funding under HEC NRPU. He has more than 40-publications, including impact factor journals, SCI and SCIE indexed journals, four book chapters, and ten Scopus indexed international conferences. His research interests include machine learning, data science, pattern recognition, and big data mining.